Monte Carlo calculational methods for the generation of events with Bose-Einstein correlations

William A. Zajc*
Physics Department, University of Pennsylvania, Philadelphia, Pennsylvania 19104
(Received 17 November 1986)

The momentum-space correlations for n bosons emitted by a source distributed in space and time are discussed in the context of intensity interferometry for identical pions. The Metropolis algorithm is used to generate events containing such correlations to all orders via a Monte Carlo technique. Direct calculation of the probability for multiparticle correlations is practicable for n-body states up to $n \sim 20$. Beyond this, a method which samples the symmetrized n-body probability must be used. It is observed that the traditional pair-correlation function is distorted for events with high phase-space density in a fashion consistent with the results of a simple model calculation.

I. INTRODUCTION

The use of intensity interferometry to study hadronic-source sizes is by now a well-established technique of high-energy physics. Typically, the two-particle correlation function is generated as a function of the relative momentum between the two (like) particles. This quantity is directly related to the Fourier transform of the density distribution for the source of these particles, thus permitting the extraction of the source size and lifetime.

In principle, the extension of such methods to more than two particles is straightforward. Experimentally, this is seldom done, since pion multiplicities in typical reactions are sufficiently low that the probability of finding three or more like-charged pions in the same region of phase space is negligible. (Given that the pion is the most abundant boson produced in hadronic reactions, I will confine my attention to pions in this paper.) Recently Willis[1] has emphasized that pion abundances in the collision of two large nuclei at high energies are sufficiently large that multipion correlations (that is, correlations that are not the product of simpler pairwise correlations) are no longer small. In the limit of very large multiplicities, the appropriate technique then becomes *speckle interferometry,* i.e., the study of phase-space clustering of large numbers of pions.

It is therefore of some interest to have a method whereby typical multipion events can be generated that explicitly exhibit all correlations induced by Bose statistics. Previous efforts[2,3] while dealing with much more complicated dynamical systems than the simple source considered here, have typically limited themselves to producing only the pairwise correlations by weighting events. This paper presents two Monte Carlo procedures for generating events of unit weight that incorporate these correlations to all orders.

The organization is as follows. Section II provides a simple introduction to the relevant features of the n-pion state. Section III describes both the algorithm used to generate the n-pion state, and methods by which the various probabilities may be efficiently calculated. Results are presented in Sec. IV, while potential methods for analyzing the correlated events are discussed in Sec. V. Conclusions and indications for future research appear in Sec. VI. Analytic results for the distortion of the pairwise correlation function by the higher-order correlations are presented in an appendix. An earlier version of this work appeared in Ref. 4; this paper extends and to some extent supersedes the material presented there.

II. n-BOSON INTENSITY INTERFEROMETRY

This section reviews the basic properties of a n-pion state arising from a source distributed in space and time. Although some portions of this discussion have been presented elsewhere (see, e.g., Ref. 5), it is included both for completeness as well as for clarity in establishing notational conventions. We begin with the canonical derivation for the case of two pions, then consider the appropriate generalizations for multipion states.

Assume that a pion of momentum p_1 is detected at x_1 and momentum p_2 at x_2. If the source of these pions has a space-time distribution given by $\rho(\mathbf{r},t) \equiv \rho(r_1)$, the probability of such an event is given by

$$\mathscr{P}_{12} = \int |\Psi_{p_1 p_2}(x_1 x_2; r_1 r_2)|^2 \rho(r_1)\rho(r_2) d^4 r_1 d^4 r_2 , \quad (1)$$

where $\Psi_{p_1 p_2}(x_1 x_2; r_1 r_2)$ is defined as the amplitude for a pion pair produced at r_1 and r_2 to register in the detectors in the prescribed fashion. In general we are unable to determine which pion was emitted at r_1 and which at r_2, so that we are required by Bose statistics to add the amplitudes for the alternative histories, as shown in Fig. 1. Regardless of the production mechanisms for the pions, if we assume that their emissions are uncorrelated and that they propagate as free particles after their last strong interaction, we have, for $\Psi_{p_1 p_2}(x_1 x_2; r_1, r_2)$,

$$\Psi_{p_1 p_2}(x_1 x_2; r_1 r_2) = \frac{1}{\sqrt{2!}} \left(e^{ip_1(x_1 - r_1)} e^{ip_2(x_2 - r_2)} + e^{ip_1(x_1 - r_2)} e^{ip_2(x_2 - r_1)} \right) . \quad (2)$$

Evaluating the squared wave function and performing the integration in Eq. (1) leads to

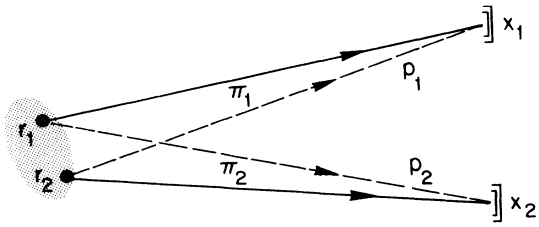

FIG. 1. The two alternate histories which contribute to the detection of a pion with momentum p_i at x_i when the pions arise from an extended source.

$$\mathscr{P}_{12}=1+|\mathscr{F}_{12}|^2 , \tag{3}$$

where

$$\mathscr{F}_{ij}\equiv\int e^{iq_{ij}x}\rho(x)d^4x, \quad q_{ij}\equiv p_i-p_j . \tag{4}$$

In all of what follows we will assume that the $\mathscr{F}_{ij}$'s are real, which in turn implies that we must have $\rho(r)=\rho(-r)$. This requirement is necessary for the efficient calculation of the multiboson state, but does not present too stringent a limitation on the allowed range of source density functions.

The extension of this approach to the n-pion state is straightforward. First we adopt the notation $\{x\}$ for the set of all x_i, $i=1$ to n, and similarly for $\{r\}$ and $\{p\}$. The n-pion state for the detection of p_i at x_i is then

$$\Psi_{\{p\}}(\{x\};\{r\}) = \frac{1}{\sqrt{n!}}\exp\left[i\sum_{i=1}^{n}p_ix_i\right]\sum_{\sigma}\exp\left[-i\sum_{i=1}^{n}p_ir_{\sigma(i)}\right], \tag{5}$$

where $\sigma(i)$ denotes the ith element of a permutation of the sequence $\{1,2,3,\ldots,n\}$, and the sum over σ denotes the sum over all $n!$ permutations of this sequence. The result of integrating over the set $\{r\}$ of all allowed source points is then given by

$$\mathscr{P}_{1,2,3,\ldots,n}=\sum_{\sigma}\mathscr{F}_{1,\sigma(1)}\mathscr{F}_{2,\sigma(2)}\cdots\mathscr{F}_{n,\sigma(n)} \tag{6}$$

$$\equiv \mathrm{per}\{\mathscr{F}\} , \tag{7}$$

where the notation per$\{\mathscr{F}\}$ denotes the *permanent* of the matrix $\mathscr{F}_{ij}$. The permanent of a matrix is similar to the determinant, except that successive permutations always contribute with the same sign, rather than alternating signs. (Had we been dealing with fermions, this result would in fact be a determinant, much like the Slater determinant of a multifermion state.)

At this point, a simple example may help clarify the formalism. Consider the source density given by

$$\rho(r)=\frac{1}{\pi^2R^3\tau}e^{-r^2/R^2-t^2/\tau^2} . \tag{8}$$

The corresponding $\mathscr{F}$ with respect to q is given by

$$\mathscr{F}(q)=e^{-(1/4)|\mathbf{q}|^2R^2-(1/4)q_0^2\tau^2} . \tag{9}$$

For a three-pion state, the general expression for the relative probability is given by

$$\mathscr{P}_{\{3\}}=1+|\mathscr{F}_{12}|^2+|\mathscr{F}_{13}|^2+|\mathscr{F}_{33}|^2 +2\,\mathrm{Re}\{\mathscr{F}_{12}\mathscr{F}_{23}\mathscr{F}_{31}\} . \tag{10}$$

Using the form for $\mathscr{F}$ found in Eq. (9) (and ignoring the temporal degrees of freedom for simplicity) we obtain, for the three-pion probability,

$$\mathscr{P}_{\{3\}}=1+e^{-(1/2)|\mathbf{q}_{12}|^2R^2}+e^{-(1/2)|\mathbf{q}_{13}|^2R^2} +e^{-(1/2)|\mathbf{q}_{23}|^2R^2} +2e^{-(1/4)(|\mathbf{q}_{12}|^2+|\mathbf{q}_{23}|^2+|\mathbf{q}_{31}|^2)R^2} . \tag{11}$$

(This is just a special form of the more general results obtained in Ref. 6.) Note that as all three relative momenta become small, the value of this expression approaches $6=3!$, reflecting the fact that the three pions are increasingly likely to be in the same state. This is of course not a property of our Gaussian source parametrization, but is true in general for the expression found in Eq. (6), since the normalization of $\rho(r)$ requires that $\mathscr{F}_{ij}(q=0)=1$.

As n_π increases, the expansion of Eq. (6) into a form like that of Eq. (11) becomes correspondingly more complex. Various powers of the $\mathscr{F}_{ij}$'s will be present (from $\mathscr{F}^0$ to $\mathscr{F}^{n_\pi}$), with the number of terms proportional to $\mathscr{F}^k$ equal to $M(k)$, where $M(k)$ is the number of ways of obtaining a permutation on n_π elements having exactly $n_\pi-k$ fixed points. In general, $M(k)$ is given by

$$M(k)=\begin{bmatrix}n_\pi\\k\end{bmatrix}d_k\approx\frac{1}{e}\frac{n_\pi!}{(n_\pi-k)!} , \tag{12}$$

where d_k is the number of *derangements*[7] of order k, given asymptotically by $d_k\approx k!/e$. For $n_\pi>2$, $k>2$, only a small fraction of the terms of order $\mathscr{F}^k$ result from the product of pairwise exchanges (this is addressed quantitatively in the Appendix). It is the purpose of the next section to develop methods capable of inducing these higher-order correlations.

Before doing so, we present a heuristic argument to describe the phase-space distribution of the n-pion state. Since the presence of k pions in a phase-space cell increases the probability of placing another pion in that cell by a factor of k, we expect a clumping of the pions on the scale of a few units of phase space. Furthermore, if the pions are fluctuating into a given cell, they must be depleting some other cell(s), leading to a domain structure in phase space. Dimensional considerations indicate that pions with $\delta p<1/R$ will be within the "range" of this enhancement factor. If we restrict ourselves to a very narrow bandwidth in $|\mathbf{p}_\pi|$, the relevant phase space is then simply the angular one, so that $\delta\theta\sim\delta p/p\sim 1/pR$, and (provided that $\delta\theta\ll 1$) the fraction of solid angle occupied by one clump (henceforth referred to as a speckle) is $\delta A\sim\pi(\delta\theta)^2/4\pi$. Thus, the number of speckles should be proportional to one over this fraction, i.e., $N_s\sim(pR)^2$.

Such considerations are well known in the context of optical speckle interferometry.[8] This technique enables one to obtain the image of a star by measuring the power spectrum of photon speckles seen (in a series of exposures

taken with a time short compared to the characteristic time for atmospheric fluctuations) in the telescope aperture. The distance scale d for speckles is given by $d=\lambda/\alpha$, where λ is the wavelength of the light and α is the aperture. For an aperture of linear dimension D, the number of speckles is $(D/d)^2$. To translate this into the particle domain, we note that $\alpha=R/S$, where S is the distance from the source to the detector and R is the size of the source. This leads to

$$N_s=\left[\frac{\rho R}{2\pi}\frac{D}{S}\right]^2,$$

which has a simple interpretation as the total number of phase-space cells intercepted by the telescope aperture.

III. MONTE CARLO METHODS FOR BOSONS

Suppose that one has an n-particle state consisting of the n momenta $\mathbf{p}_i$, $i=1$ to n, where the $\mathbf{p}_i$ are each picked independently from some distribution $dn/d\mathbf{p}$. The results of the previous section demonstrate that if the n particles are like bosons, the n-particle state is then no longer given by n samples of the single-particle momentum distribution. That is, the presence of a particle in some region of phase space makes it more likely that another particle will be found "nearby," where the scale for "nearness" is set by the (inverse) source size. This section will describe the basic algorithm used to induce such correlations on a set of initially independent vectors.

The approach used is the standard Monte Carlo technique due to Metropolis.[9] This is a general method which allows one to generate an ensemble of n-body configurations according to some probability density. That is, the probability of a given configuration in the ensemble is precisely that given by the probability density used to generate "successive" configurations. In the context of the present problem, the algorithm may be stated as follows.

FOR $i=1,n_\pi$

$\mathbf{p}_i' \leftarrow dn/d\mathbf{p}$

$P_{\text{old}}=\mathscr{P}\{p_1\cdots\mathbf{p}_i\cdots\mathbf{p}_{n_\pi}\}$

$P_{\text{new}}=\mathscr{P}\{p_1\cdots\mathbf{p}_i'\cdots\mathbf{p}_{n_\pi}\}$

ACCEPT $\mathbf{p}_i'$ with probability $=\min\{1,P_{\text{new}}/P_{\text{old}}\}$

NEXT i

where the probability of a given set of momenta is written as $P_{\text{old}}=\mathscr{P}\{p_1\cdots\mathbf{p}_i\cdots\mathbf{p}_{n_\pi}\}$. [Its value is given by Eq. (6).] Since a straightforward application of this expression requires the evaluation of $n!$ terms, it is obvious that a more intelligent approach will be necessary before applying the Metropolis algorithm to states with $n_\pi \gtrsim 10$. Various methods of circumventing this problem, and therefore avoiding the factorial growth in calculating $\mathscr{P}\{p_1\cdots\mathbf{p}_i\cdots\mathbf{p}_{n_\pi}\}$, will now be discussed.

There is a general algorithm for the efficient calculation of permanents due to Ryser. The method here is a modification of Ryser's algorithm given by Nijenhuis and Wilf[10] which requires for an $n\times n$ permanent on the order of $n2^{n-1}$ operations rather than the $n\cdot n!$ operations implied by a straightforward calculation according to the definition of Eq. (6). Their algorithm may be stated as

$$\text{per}\{\mathscr{F}\}=(-1)^{n-1}2\sum_S(-1)^{|S|}\prod_{i=1}^{n}\left[f_i+\sum_{j\in S}\mathscr{F}_{ij}\right], \tag{13}$$

where

$$f_i=\mathscr{F}_{i,n}-\tfrac{1}{2}\sum_{j=1}^{n}\mathscr{F}_{ij}, \tag{14}$$

S denotes all subsets of the sequence $\{1,2,\ldots,n-1\}$ and $|S|$ is the number of elements in a given subset. Essentially, this prescription forms all n products of the row sums of $\mathscr{F}$, with appropriate minus signs to remove terms that appear more than once.

Even though the above algorithm for an $n\times n$ permanent is faster by a factor of roughly $2(ne/2)^n$ over direct computation of the permanent, the execution time still grows exponentially with n_π. Efficient calculation for states with $n_\pi \gtrsim 20$ require a different approach, based on *sampling* the probability density given by Eq. (6). This method, first introduced by Ceperley *et al.*[11] can be viewed as a random walk in permutation space as well as momentum space for the system. Alternatively we may think of it as using the Metropolis algorithm to sample each term of Eq. (6) with a probability for a given term proportional to its average value. The sampling procedure may be written as follows.

FOR $i=1,n_\pi$

First move in momentum space:

$p_i' \leftarrow dn/d\mathbf{p}$

$P_{\text{old}}=\mathscr{P}\{p_1\cdots\mathbf{p}_i\cdots\mathbf{p}_{n_\pi}\}$

$P_{\text{new}}=\mathscr{P}\{p_1\cdots\mathbf{p}_i'\cdots\mathbf{p}_{n_\pi}\}$

ACCEPT $\mathbf{p}_i'$ with probability $=\min\{1,P_{\text{new}}/P_{\text{old}}\}$

FOR $k=1,n_\pi,k\neq i$

Now move in permutation space:

$P_{\text{old}}=\mathscr{F}_{i,\sigma(i)}\mathscr{F}_{k,\sigma(k)}$

$P_{\text{old}}=\mathscr{F}_{i,\sigma(k)}\mathscr{F}_{k,\sigma(i)}$

SWAP $\sigma(i)\leftrightarrow\sigma(k)$ with probability

$=\min\{1,P_{\text{new}}/P_{\text{old}}\}$

NEXT k

NEXT i

In the above we have written $\sigma^{-1}(i)$ to denote the inverse

permutation, such that $\sigma^{-1}[\sigma(i)]=i$. Note that the trial permutation is simply given by pairwise exchange of the current permutation. In this sense, we have a *connected* random walk in permutation space. The only particular advantage to this scheme is in terms of computation time, since all but two of the factors in a given term of $\mathcal{F}_{1,\sigma(1)}\mathcal{F}_{2,\sigma(2)}\cdots\mathcal{F}_{n,\sigma(n)}$ remain unchanged, so that all but the affected factors cancel in forming the ratio of P_{new} to P_{old}. If execution time (and numerical accuracy) were not a consideration, an entirely new permutation could be selected for each test.

To visualize how the pairwise exchange of permutations explores the various terms in the expansion of Eq. (6), we present in Fig. 2 a schematic representation of one sweep for $n_\pi=9$. Each pion momentum vector $\mathbf{p}_i$, $i=1,9$, is represented as a point in (angular) phase space. The terms $\mathcal{F}_{i,\sigma(i)}$ corresponding to a given permutation σ are shown as arrows from pion i to pion $\sigma(i)$, except for unit permutations $\mathcal{F}_{ii}$, which are drawn as circles around the ith pion. While the largest *single* term in the expansion of Eq. (6) is of course the unit permutation $\sigma(i)=i$, the *number* of terms corresponding to higher-order permutations increases according to Eq. (12). Those more complicated configurations that "minimally span" the space with the "metric" $\mathcal{F}_{ij}$ are then those that are preferentially considered by the Metropolis algorithm. Figure 2 shows how pairwise exchanges can lead to a permutation sequence that produces links that make explicit the clustered nature of the pions in this event.

Finally, it is interesting to note that the historical origins of generating Bose-correlated states via Monte Carlo simulation date back to the earliest work in this field, that of Goldhaber, Goldhaber, Lee, and Pais.[12] These authors evaluated two-particle distribution functions over multiparticle states by evaluating integrals over the correlations induced by Bose statistics. They considered an extended space-time source quite similar to the one chosen here (see below), while their integration method consisted of the usual "hit-or-miss" technique. The Metropolis procedure allows us to evaluate the same sort of distribution functions directly over the events themselves; but in reality consists only of another prescription for evaluation of the phase-space integrals encountered in these calculations.

IV. RESULTS

In this section we present some of the properties of the Bose states generated by techniques described above, and examine the convergence properties of the two algorithms. Results obtained by exact evaluation of the permanent with Eq. (13) will be referred to as the RWN result (for Ryser, Wilf, and Nijenhuis), while those obtained by the Monte Carlo evaluation of the permanent will be labeled as CCK results (for Ceperley, Chester, and Kalos). First we will briefly discuss the choice of momenta and source size appropriate for heavy-ion collisions at proposed colliding-beam facilities.[13]

Simple considerations lead one to expect that central collisions of equal-mass ions produce (in the central rapidity region) A times the particle density for pp collisions at the same $\sqrt{s}$ per nucleon,[14] where A is the atomic mass of one of the ions. Given that typical rapidity densities for like-pion production in pp collisions at $\sqrt{s}\sim 100$ GeV is about one, we then expect on the order of A like pions per unit of rapidity for colliders in the 100-GeV per nucleon range. Similarly, the transverse-momentum spectrum in the central region is expected (in the absence of dramatic new effects) to resemble that obtained in pp colliders, i.e.,

$$\frac{dn}{dp_t}\propto p_t e^{-2p_t/\langle p_t\rangle}, \tag{15}$$

with $\langle p_t\rangle\sim 300$ MeV/c. Finally we assume that source sizes will scale as $R\sim A^{1/3}$ fm (at least in the transverse

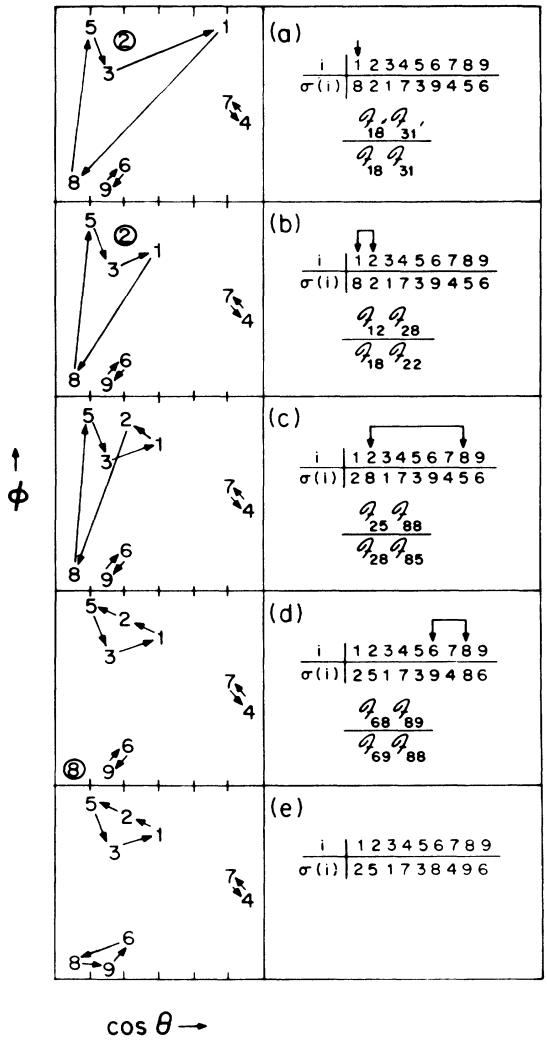

FIG. 2. A schematic representation of the RWN algorithm. The left-hand side contains a series of configurations, updated first in momentum space (a) and (b), then in permutation space (c)—(e). On the right-hand side is the current permutation σ, and the ratio of probabilities that determines the acceptance of this step. The arrows over the permutation sequence indicate the exchanges or updates for generating the next configuration. See text for further details.

dimensions), leading to $R \sim 6$ fm for U-U collisions.

It is not our purpose here to provide a realistic parametrization of the complicated source dynamics expected in a very energetic heavy-ion collision. Instead, guided by the above considerations, we wish to select source parameters appropriate to the characteristic scales of the problem (there are more than one, as we shall see below). Therefore, we will take our canonical source as given by Eq. (8), with $R=\tau=6$ fm (thereby completely ignoring the issue of longitudinal growth[15]). We assume an isotropic source, but restrict all pion momenta to the region $|\mathbf{p}_\pi| = 300 \pm 15$ MeV$/c \equiv p_0 \pm \Delta p$, so that the actual value of τ is not important. The value chosen for the range in the magnitude of momenta is such that $\Delta p \sim 1/R$, consistent with the discussion of Sec. II. These parameters will remain fixed as the number of pions in an event is varied from $n_\pi = 10$ to $n_\pi = 500$. These values nicely span the actual number of pions expected (~ 70, in the central four units of rapidity for 100 GeV U + 100 GeV U collisions and the above-mentioned value of Δp). This then allows us to study the efficiencies of the CCK and RWN algorithms as a function of n_π in the regions of interest for future applications.

In order to assess the performance of the two algorithms, a quantitative measure of the Bose correlations is required. While ultimately we will be interested in event-by-event information, for now we will consider a measure evaluated over a subsample of the ensemble of events generated by the Metropolis method. Specifically, the pair-correlation function $C_2(|\mathbf{q}|)$, given by

$$C_2(|\mathbf{q}|) \equiv \frac{\langle dn/d\mathbf{q} \rangle_{\text{corr}}}{\langle dn/d\mathbf{q} \rangle_{\text{rand}}} \equiv \frac{A(\mathbf{q})}{B(\mathbf{q})} , \tag{16}$$

will be calculated as a function of the number of sweeps from the initial configuration. [The pairs used in the above expression are restricted to $q_0 < 20$ MeV$/c$, so that $C_2(|\mathbf{q}|)$ may be regarded as a function of $\mathbf{q}$ only.] In the above expression, the angular brackets refer to averages performed over the relative momentum density of a large number of events. The events in the numerator are some set of sequential events generated via the Metropolis procedure, $A(\mathbf{q})$, while the denominator is simply the same average evaluated for randomly distributed pions, $B(\mathbf{q})$. If in fact this subsample is distributed according to the permanent probability distribution given by Eq. (6), the expected form for $C_2(|\mathbf{q}|)$ is

$$C_2(|\mathbf{q}|) = 1 + |\mathcal{F}(\mathbf{q})|^2 , \tag{17}$$

where $\mathcal{F}$ is given by Eq. (9). (This form assumes that the phase-space density of pions is much less than unity. Corrections for higher densities are discussed later in this section and in the Appendix.) Thus, by fitting $C_2(|\mathbf{q}|)$ to the form

$$C_2(|\mathbf{q}|) = \alpha(1 + \lambda e^{-q^2 R_f^2/2}) , \tag{18}$$

we can examine the dependence of the parameters λ and R_f on the number of sweeps, and thereby determine the convergence properties of the CCK or RWN algorithm.

Figures 3 and 4 show the dependence of R and λ on the number of sweeps for $n_\pi = 10$ and $n_\pi = 15$, respectively,

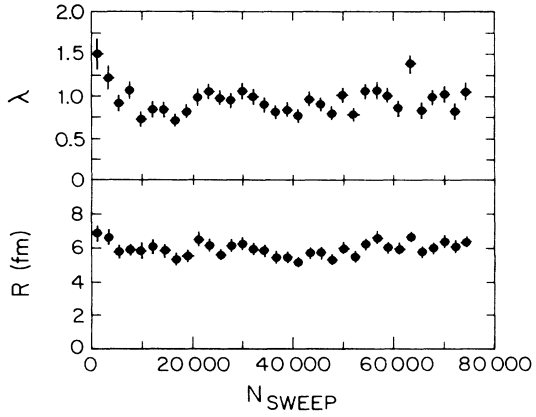

FIG. 3. The dependence of R and λ in Eq. (18) on the number of sweeps for $n_\pi = 10$ using the RWN algorithm.

both using the RWN algorithm. It is clear that fewer than 1000 sweeps are necessary to obtain the equilibrium values of these parameters, and that the values extracted are consistent with those used in generating these events. Furthermore, the value of the parameters are stable with respect to the number of sweeps, so that the effect of an "abnormal" event does not persist for many sweeps [the fluctuations in λ for the $n_\pi = 15$ case result from the very small number of pairs used to generate $C_2(|\mathbf{q}|)$, cf. Fig. 8].

Such stability is not present in the CCK method for this system, as may be seen by examining the corresponding distributions (for $n_\pi = 15$) presented in Fig. 5. While the average value of R and λ may be correctly represented, the fluctuations clearly dominate the signal. This results in part from the fitting procedure used to obtain these parameter histories, where Poisson-distributed, uncorrelated errors are assumed. Examination of one of the temporary $C_2(|\mathbf{q}|)$'s generated by this algorithm (Fig. 6) show that this is not the case: the error bars ascribed by the usual $\sqrt{n}$ are obviously too small. This is in contrast with the corresponding distributions for the RWN procedures (Figs. 7 and 8), which are clearly well behaved,

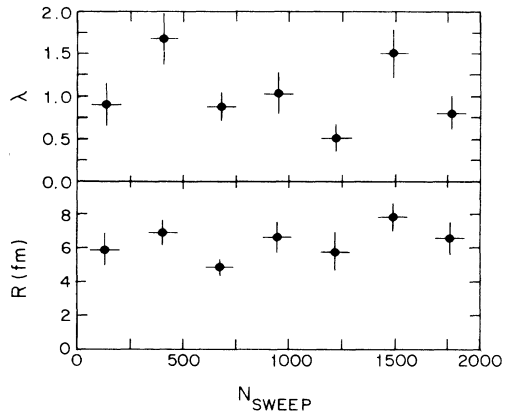

FIG. 4. The dependence of R and λ in Eq. (18) on the number of sweeps for $n_\pi = 15$ using the RWN algorithm.

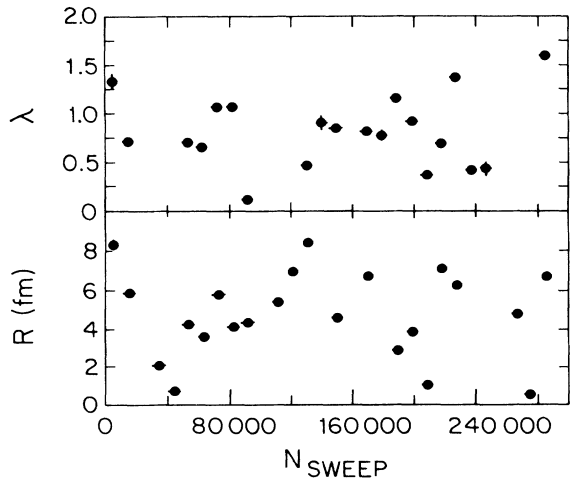

FIG. 5. The dependence of R and λ in Eq. (18) on the number of sweeps for $n_\pi = 15$ using the CCK algorithm.

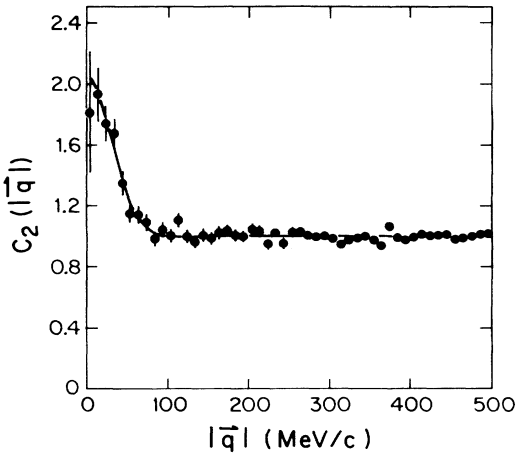

FIG. 7. The correlation function $C_2(|\mathbf{q}|)$ generated via the RWN algorithm for $n_\pi = 10$.

even though the RWN function contains far fewer events than the CCK function (~ 240 vs $\sim 10^4$). Figure 9 shows that the long-term (3×10^5 events) averages using the CCK method do indeed converge to a correlation function of the proper shape, although again the fluctuations greatly exceed those expected from Poisson statistics.

It is natural to assume that these fluctuations result from nonergodicity in the sampling of the permanent required by the CCK approach. What is surprising to learn is that increasing the pion density (that is, increasing n_π at fixed p_0 and R) improves the effectiveness of the sampling procedure, despite the factorial growth in the number of terms to be visited. The empirical evidence for this is presented in top and middle portions of Figs. 10–12. (Note that the horizontal axis is different for the three sets of figures.) It is readily apparent that as n_π increases, the fluctuations in the fitted parameters decrease.

This may be understood in terms of a "hopping probability" between classes of permutations. The considerations of Sec. II leading to Eq. (12) indicate that number of higher-order terms in $\mathcal{F}$ increases very rapidly. However, in order to sample them freely, we must have

$$\begin{bmatrix} n_\pi \\ k+1 \end{bmatrix} d_{k+1} \mathcal{F}^{k+1} \sim \begin{bmatrix} n_\pi \\ k \end{bmatrix} d_k \mathcal{F}^k \tag{19}$$

for as many values of k as possible. Using the asymptotic relation $d_k \approx k!/e$, this can be reduced to $(n_\pi - k)\mathcal{F} \sim 1$. Finally, it is straightforward to show that the angular average of $\mathcal{F}_{ij}$ (for a random distribution) is $\sim 1/(pR)^2$, so that a "good" calculation will satisfy $n_\pi - k \sim (pR)^2$. Since we are moving in permutation space by pair exchange, the most crucial steps will be in moving away from low values of k, leading to the condition $n_\pi \sim (pR)^2 \sim 80$ for our chosen values of p and R. Inspection of Fig. 10 supports these arguments: there is a qualitative change in the stability of the fit parameters as n_π is increased from 15 to 100, as expected from Eq. (19). This change occurs just as the fraction of terms involving

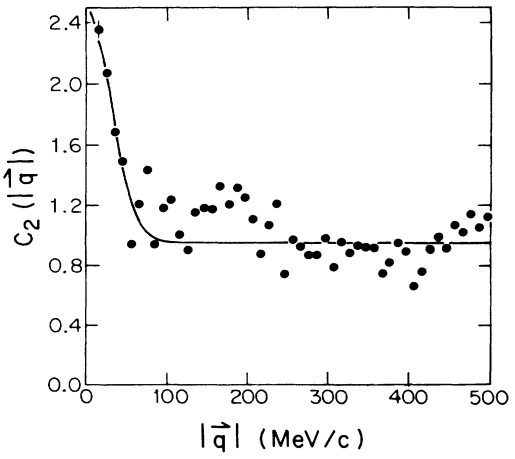

FIG. 6. The correlation function $C_2(|\mathbf{q}|)$ generated via the CCK algorithm for $n_\pi = 15$.

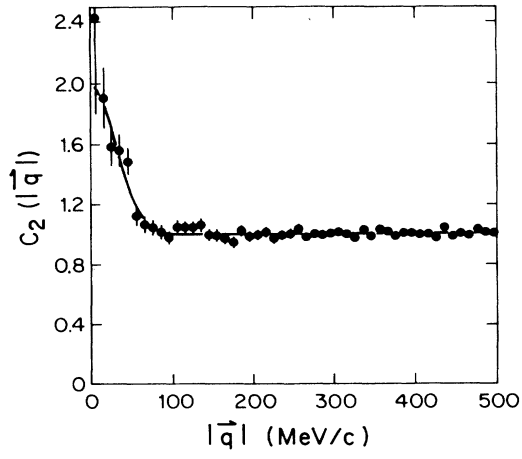

FIG. 8. The correlation function $C_2(|\mathbf{q}|)$ generated via the RWN algorithm for $n_\pi = 15$.

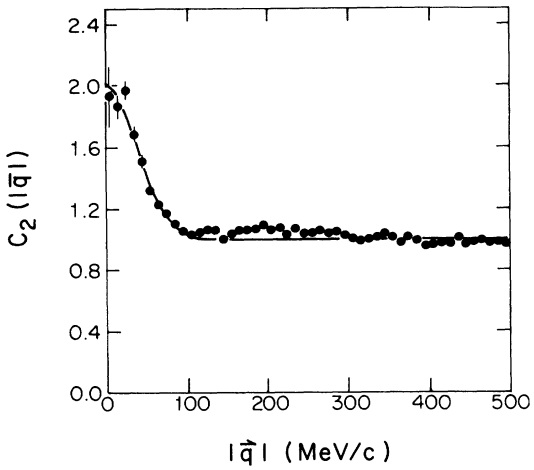

FIG. 9. The correlation function $C_2(|\mathbf{q}|)$ generated via the RWN algorithm for $n_\pi=15$, averaged over $300K$ events.

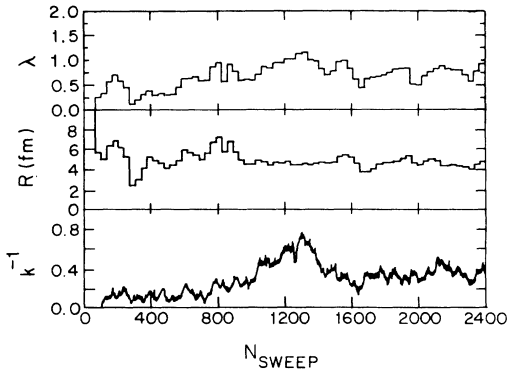

FIG. 11. The sweep history of λ, R, and k using the CCK algorithm for $n_\pi=250$.

higher-order permutations becomes large, as shown in Fig. 13. This figure plots the fraction of permutations of length 3 or greater versus the number of pions (these are the permutation terms that cannot be reproduced by algorithms that compute only the product of pairwise exchanges). Note that this figure shows not simply the number of such permutations as a function of n_π, but rather their importance (i.e., weighted by the appropriate factors of $\mathcal{F}_{ij}$) in the expansion of the permanent.

The condition that $n_\pi \sim (pR)^2$ is equivalent to a requirement of about one pion per phase-space cell. Here we have assumed that the momentum band is restricted to $\Delta p \sim 1/R$, so that the number of phase-space cells

$$V 4\pi p^2 \Delta p/(2\pi)^3 \sim (pR)^2 .$$

One consequence of such high phase-space densities is that the simple form of Eq. (17) is lost. In the Appendix it is shown that the characteristic result of the high-density limit[16] is to reduce the values of R and λ extracted by fitting the pair-correlation function to the form of Eq. (18). This effect is clearly visible in Figs. 10–12. For instance, the fully developed n-body correlations for a source with $n_\pi=500$, $R=6$ fm, $p_0=300$ MeV/c lead to a *two*-body correlation function whose width corresponds to a fitted radius of $R_{\rm fit}\approx 3$ fm (Fig. 14).

A second consequence of high phase-space densities is that the expansion of the permanent is increasingly dominated by higher-order permutations. It is a simple matter during the execution of the RWK algorithm to monitor the length of each cycle in the current permutation sequence. Empirically, it is observed that the fraction of cycles of length greater than two is roughly given by the expression

$$f_{>2}\approx \ln\left[1+\frac{n_\pi}{n_\pi+160}\right] . \tag{20}$$

Although the form of this dependence is suggestive (the parameter 160 is of the same order-of-magnitude as the number of phase-space cells), we are unable to provide an argument leading to this result. Nonetheless, the implication is clear: modeling the pion correlations to high accuracy in heavy-ion collisions at high energies will require the inclusion of higher-order correlations.

We close this section by comparing the efficiencies of

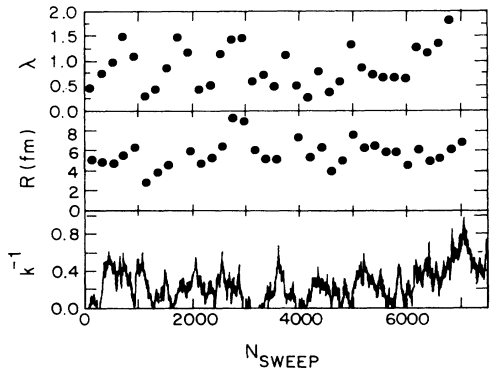

FIG. 10. The sweep history of λ, R, and k using the CCK algorithm for $n_\pi=100$.

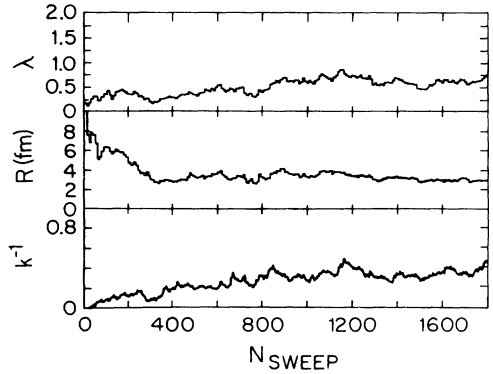

FIG. 12. The sweep history of λ, R, and k using the CCK algorithm for $n_\pi=500$.

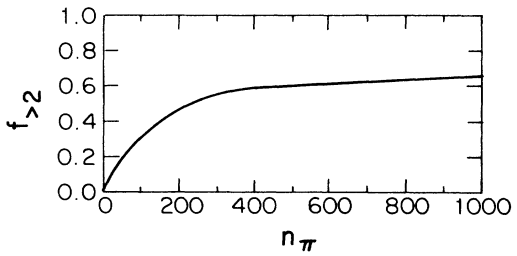

FIG. 13. The fraction of permutation cycles of length 3 or greater as a function of n_π.

the RWN and CCK algorithms as a function of n_π. Timing tests[17] indicate that the time per sweep for the RWN method is given by

$$\tau_{\mathrm{RWN}} \approx (10 \text{ sec}) \times n_\pi 2^{n_\pi - 18} , \tag{21}$$

while the time per sweep for the CCK calculations is

$$\tau_{\mathrm{CCK}} \approx \left[\frac{n_\pi}{50} \right]^2 \text{sec} . \tag{22}$$

Even though the previous analysis indicates that the CCK algorithm requires far more sweeps than the RWN method to obtain ergodicity, it is clear that the power law must win out over the exponential at some value of n_π. For example, assume (very conservatively) that the CCK algorithm requires 1000 times as many sweeps to generate events of statistical significance comparable to those of the RWN method. Then the above scaling laws indicate that the CCK calculation is more efficient for $n_\pi \gtrsim 18$. It is fortunate that this trade-off occurs precisely where it is most needed, i.e., at the point where RWN-based calculations being to take $\sim$24 hr of CPU time. Given that the RWN algorithm requires an order of magnitude more time for every 3 or 4 pions, it is obvious that even extraordinary advances in computational speed prevent its extension to states with $n_\pi > 50$.

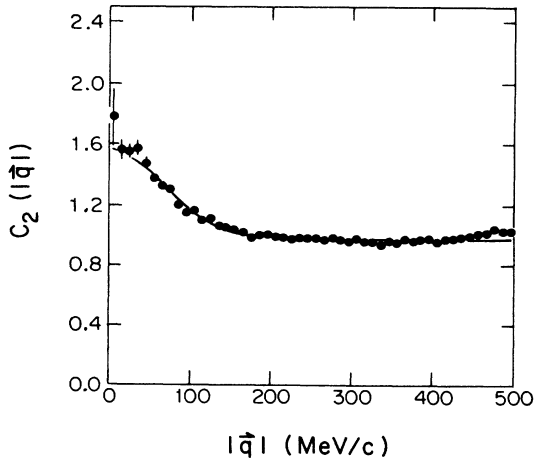

FIG. 14. The two-body correlation function $C_2(|\mathbf{q}|)$ for $n_\pi = 500$. The fitted parameters are $\lambda = 0.6$, $R = 2.9$ fm.

V. GLOBAL EVENT FEATURES AND IMAGE RECONSTRUCTION

This section examines the fluctuations in phase space of the Bose-correlated states from the CCK algorithm, and briefly discusses how such information may be used to extract details of the source distribution. The heuristic considerations of Sec. II lead to the expectation of "large" fluctuations in the phase-space distribution of the pions in these events. Visible evidence for this is presented in Fig. 15, which compares the angular phase-space distributions for a typical correlated and uncorrelated event. It is clear that the Bose-correlated event is "clumpier" than the randomly generated event.

To determine the significance of the fluctuations in Fig. 15, we have calculated the quantity

$$\tilde{\chi}^2 \equiv \frac{1}{N_B} \sum_{i=1}^{N_B} \frac{(n_i - \bar{n})^2}{\bar{n}} , \tag{23}$$

where n_i is the number of pions in the ith phase-space bin, N_B is the number of phase-space bins, and $\bar{n}$ is the average occupancy $\bar{n} = n_\pi / N_B$. If each bin contains k phase-space cells, we expect the distribution of n_i to be given by the negative-binomial distribution for k cells,

$$\mathscr{P}(n) = \binom{n+k-1}{n} \beta^n (1-\beta)^k , \tag{24}$$

with $\beta = \bar{n}/(\bar{n}+k)$, leading to

$$\tilde{\chi}^2 = 1.0 + \frac{\bar{n}}{k} . \tag{25}$$

Using phase-space bins of size $d(\cos\theta) d\Phi = 0.2 \times 0.1 (2\pi)$, we find for the correlated event in Fig. 15 that $\tilde{\chi}^2 = 3.25 \Rightarrow k = 2.2$. The statistical significance of this result may be estimated by standard means[18] to be roughly 11σ, indicating that this event is very unlikely to be a chance fluctuation of an uncorrelated distribution.

The value obtained for k indicates that each of the 100 bins used in the above analysis contains $\sim$2.2 phase-space cells. Long-term averages over k indicate that the actual value of k is 3.0 ± 0.2, so that the total number of cells available to the pions in our events is $\sim$300, rather than $(p_0 R)^2 \sim 80$ previously estimated. This is not unexpected, since the extended nature of the Gaussian source presumably leads to a larger effective coordinate-space volume V in the number of states $V d^3p/(2\pi\hbar)^3$.

The dependence of k^{-1} on the number of sweeps is shown in the lower portion of Figs. 10–12 for $n_\pi = 100$–500. After a number of sweeps sufficient to build in the Bose correlations, the average value of k^{-1} is roughly 0.33, independent of n_π, although once again the fluctuations of this quantity increase with decreasing pion numbers. The fact that the value of k is independent of n_π indicates that the fluctuations scale with $\bar{n}$ as indicated by Eqs. (23) and (25), just as one would expect from Bose statistics.

It is of interest to examine the complete probability distribution for cell multiplicities, shown in Fig. 16, again for events with $n_\pi = 500$. The smooth curves correspond to a negative binomial with $k = 3.08$. The error bars in this figure have been increased by a factor of 6 relative to

those calculated assuming Poisson statistics on the number of entries in each bin. Such a scaling, of course, does not change the fitted value of the k, but does scale the error on this quantity to the value $k=3.08\pm0.22$. The factor of 6 is chosen to produce a χ^2 per degree of freedom of order unity, providing us with further evidence that successive events generated via the CCK algorithm are not statistically independent, but instead have a "correlation length" in event space of order 6—10 events. (This conclusion is clearly a strong function of n_π, as indicated by Figs. 10—12.) It is important to note that the negative-binomial shape for the multiplicity distribution, along with an appropriate value for k, are produced *automatically* by the Bose correlations resulting from the finite source size; it is not an additional input into our event-generating procedure. We regard this, and the scaling of the multiplicity fluctuations with $\bar{n}$, as stringent tests for the applicability of our model.

We now discuss the extraction of source parameters from the Bose events. To motivate this, we consider the expression for the signal-to-noise ratio obtained for speckle interferometry in the optical regime:[8]

$$\frac{S}{N}=N_{\rm ev}{}^{1/2}n_{\pi/s}N_s{}^{1/2}\ , \tag{26}$$

where $N_{\rm ev}$ is the number of frames of data, or events, $n_{\pi/s}$ is the number of bosons per speckle (pions in our case), and N_s is the number of speckles per event. (The ratio S/N is defined as the rms value of the image density to the error on the same, and thus corresponds roughly to the ratio of the R to the error in measuring the radius.) Following the considerations of Sec. II, the expression for S/N may be written as

$$\frac{S}{N}=\left[N_{\rm ev}\left[\frac{2\pi}{p_0R}\right]^2 n_{\rm pairs/ev}\right]^{1/2}\ , \tag{27}$$

where $n_{\rm pairs/ev}$ is the number of boson pairs per event. Thus, the determination of the source parameters via the canonical speckle methods depends on the total number of pairs of relative momentum measured, just as for the usual two-particle correlation function. Note also that the expression for the signal-to-noise ratio is inversely proportional to the pion phase-space density.

These results may be understood by recalling that optical speckle interferometry is simply a special case of intensity interferometry, which exploits the correlations $\langle I_1I_2\rangle$ between the intensities of the received wave fronts. For instance, the Fourier transform of the image-plane correlation function

$$C_1(x_1)\equiv\frac{\langle I(x+x_1)I(x)\rangle-\langle I\rangle^2}{\langle I\rangle^2} \tag{28}$$

is equal to the autocorrelation of the source function, as shown in Ref. 8. Translated into the particle regime, this

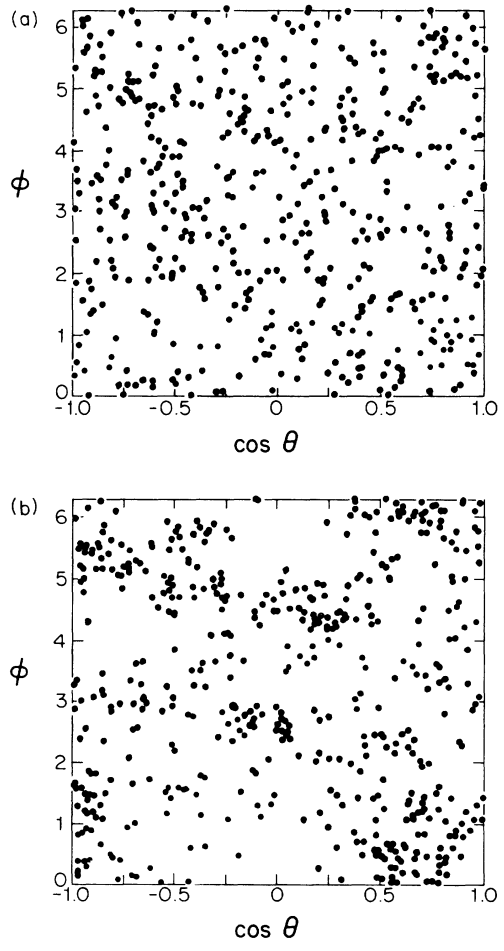

FIG. 15. Angular phase-space distributions with $n_\pi=500$ for (a) uncorrelated and (b) Bose-correlated events. The points in (b) are assumed to be emitted from a source of (Gaussian) radius=6 fm with $p_0=300$ MeV/c.

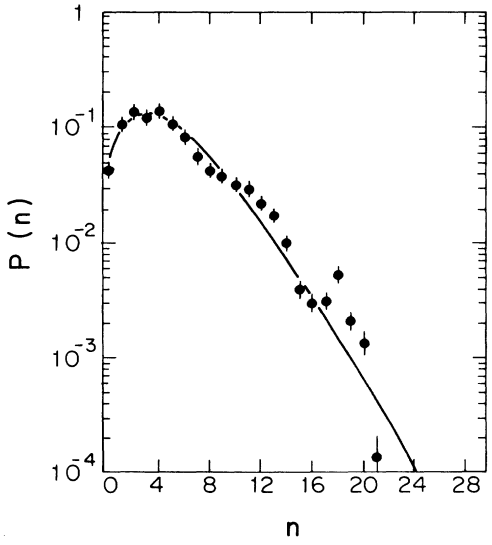

FIG. 16. The probability distribution for cell occupancies in Bose-correlated events with $n_\pi=500$, along with a fit to a negative-binomial distribution. The errors have been increased by a factor of 6 relative to those calculated assuming Poisson statistics.

result becomes

$$\int e^{-iqr}\frac{\langle n(p+q)n(p)\rangle-\langle n\rangle^2}{\langle n\rangle^2}dq = \int \rho(r+u)\rho(u)du\ , \quad (29)$$

which is just the usual result for the two-pion correlation function, written in an integral form. It is clear that this equivalence results from the intrinsic nature of measuring intensity correlations; the boson-operator expansion of $\langle I_1 I_2\rangle$ corresponds to two-particle correlations. If additional information is to be extracted from the n-boson state, it must be done through higher-order correlations. For instance, three-body correlations contain information concerning the relative phases of the pions [as suggested by Eq. (10)] which is completely unavailable to the two-particle analysis. Steps in this direction have already begun for both heavy-ion collisions[19] and e^+e^- data.[20,21]

VI. CONCLUSIONS

A formalism has been presented for describing the momentum correlations induced by an extended source of pions. It has been shown that a Metropolis-based Monte Carlo algorithm allows one to use this formalism to produce an ensemble of n-pion events containing these correlations. For small values of n_π, the most efficient approach employs a direct calculation of the n-body permanent, using an algorithm due to Ryser, as modified by Wilf and Nijenhuis. For $n_\pi \gtrsim 20$, a Monte Carlo sampling of the permanent has been shown to be most efficient. Finally, various quantities such as the number of speckles, the signal-to-noise ratio, and the time scale for ergodic behavior have been shown to depend on the dimensionless quantity $pR/\hbar$.

Many interesting subjects remain for further study. The inclusion of lifetime determinations (at least as important in understanding actual collision features) in addition to size measurements has not been discussed. Related to this are the results of thermal smearing, or more properly, introduction of the correct momentum spectrum $dn/d\mathbf{p}$, perhaps by applying this algorithm for like-particle symmetrization to the results of various Monte Carlo predictions of nuclear events. Finally, the optimal method for extraction of source parameters from the multipion events remains to be determined. In principle, all of these questions may be investigated by an extension of the methods presented here.

We conclude with two observations. First it is important to realize that the expected events from future heavy-ion colliders such as the Brookhaven RHIC will explore Bose correlations in an intermediate regime. By this we mean that the "wave" term [$\bar{n}/k$ in Eq. (25)] will be of the same importance as the "particle" term (1.0 in the same equation). It is this interplay between shot-noise and boson clumping that leads to the smeared appearance of phase plots such as Fig. 15. It is not unreasonable to suggest that new techniques will be required to extract source parameters from events of this type. Second we wish to stress that regardless of the technique employed, it is essential that the systematic variation with n_π of R and λ (as measured by the two-particle correlation function) can be understood and corrected for. Were this not done, one would conclude that events with higher pion multiplicities are both denser (smaller R) and more coherent (smaller λ). The methods developed in this paper allow one to study and separate purely statistical effects from more complicated dynamical ones.

ACKNOWLEDGMENTS

It is a pleasure to acknowledge essential conversations with W. Willis concerning speckle interferometry, with T. Humanic regarding modeling of the pion source, and with P. Edelman concerning combinatorial esoterica too numerous to enumerate. The support of S. Frankel and the Aspen Center for Physics is also gratefully acknowledged. This work was conducted under DOE Contract No. DE-AC02-76-ERO-3071.

APPENDIX

This appendix contains calculational details of the pair-correlation for a multipion source. More properly, we will explore the variation with n of the quantity $\mathrm{Tr}[n(\mathbf{p}_1)n(\mathbf{p}_2)\rho_\pi^{(n)}]$, where $\rho_\pi^{(n)}$ is the n-pion density matrix appropriate to an extended space-time source. This will be done using a formalism presented in Ref. 5, along with an explicit representation for both the spatial density of the source and for the single-particle momentum distribution. For convenience and clarity we will ignore temporal degrees of freedom, and will avoid three-vector notations. Thus, dx denotes d^3x, $\mathbf{k}\cdot\mathbf{x}$ is written as $k\cdot x$, etc.

Multipion states $|x_1,x_2,\ldots,x_n\rangle$ are created by repeated operation of the single-particle creation operator

$$\phi^\dagger(\mathbf{x}) \equiv \int \frac{dk}{(2\pi)^{3/2}} e^{ikx} f(k) a_k^\dagger\ , \quad (A1)$$

where $f(k)$ will be related to the single-particle momentum distribution below and $a_k^\dagger$ is the standard momentum-space creation operator. Single-particle states in this scheme have the inner product

$$\langle x_i | x_j\rangle = f_{ij}\ , \quad (A2)$$

where f_{ij} is given by

$$f_{ij} = \int \frac{dk}{(2\pi)^3} |f(k)|^2 e^{-ik(x_i-x_j)}\ . \quad (A3)$$

For multipion states, the normalization reflects the finite extent of the single-particle wave packets:

$$\langle x_1,\ldots,x_n | x_1,\ldots,x_n\rangle = \mathrm{per}\{f\}\ , \quad (A4)$$

where f is the matrix of f_{ij}'s given by Eq. (32) and per denotes the permanent of this matrix.

Assuming the pions are independently created by an extended source with a density distribution $\rho(x)$, the n-pion density matrix may then be written as

$$\rho_\pi^{(n)}=N_{(n)}{}^{-1}\int dx_1\cdots dx_n\rho(x_1)\cdots\rho(x_n)\,|\,x_1,\ldots,x_n\rangle\langle x_1,\ldots,x_n\,|\ , \tag{A5}$$

where $N_{(n)}$ is a normalization constant determined by the requirement that $\mathrm{Tr}(\rho_\pi^{(n)})=1$:

$$N_{(n)}=\int \mathrm{per}\{f\}dx_1\cdots dx_n\ . \tag{A6}$$

A one-particle state then has the momentum distribution

$$\frac{dn}{dp}=\mathrm{Tr}[\rho_\pi^{(1)}n(p)]=\frac{|f(p)|^2}{(2\pi)^3}\ , \tag{A7}$$

where $n(p)=a_p^\dagger a_p$. We may regard this as the low-density limiting definition of the single-particle momentum distribution, since for higher multiplicities details of the source distribution modify dn/dp. For example, it is simple to calculate that

$$\frac{dn^{(2)}}{dp_1}=\mathrm{Tr}[\rho_\pi^{(2)}n(p_1)]=2N_{(2)}{}^{-1}\frac{|f(p_1)|^2}{(2\pi)^3}\left[1+\int dp_2\frac{|f(p_2)|^2}{(2\pi)^3}|\mathscr{F}(p-p_2)|^2\right], \tag{A8}$$

where $\mathscr{F}(p_{ij})$ is again the Fourier transform of $\rho(x)$, as given below in Eq. (A10) and analogous to Eq. (4). (This result is just the integral of $dn^{(2)}/dp_1dp_2$ over the unobserved second momentum vector p_2.) In Ref. 5 it is argued on general grounds that such correction terms for collisions of heavy ions with atomic mass A must be of order $1/A$, and therefore small for the reactions of interest to those authors. This result, based as it is on simple uncertainty-principle arguments, must remain true for the specific spatial and momentum distributions we employ below to parametrize the correction terms. What has changed is the extension of these calculations to the high-pion density limit, where the *number* of correction terms is very large.

To see this we will first calculate the corrections to the two-particle correlation function induced by the presence of a third pion, then extend these results to the case of a many-pion state. (Similar results for the three-pion case are presented in Refs. 19 and 21.) For the sake of definiteness, we will use the distributions

$$\frac{dn}{dp}=\frac{|f(p)|^2}{(2\pi)^3}=\frac{1}{(2\pi p_0{}^2)^{3/2}}e^{-p^2/2p_0{}^2}\ ,$$
$$\rho(x)=\frac{1}{(\pi R^2)^{3/2}}e^{-x^2/R^2}\ . \tag{A9}$$

These Fourier transforms of these distributions will be needed in what follows:

$$f_{ij}=e^{-(p_0{}^2/2)(x_i-x_j)^2}\ ,$$
$$\mathscr{F}_{ij}\equiv\int e^{ix(p_i-p_j)}\rho(x)dx=e^{-(R^2/4)(p_i-p_j)^2}\ . \tag{A10}$$

The two-particle correlation function for a three-particle state is then given by the expression

$$\frac{N_{(3)}}{6}\frac{\dfrac{dn^{(3)}}{dp_1dp_2}}{\dfrac{dn^{(1)}}{dp_1}\dfrac{dn^{(1)}}{dp_2}}=\int dp_3\frac{|f(p_3)|^2}{(2\pi)^3}[1+|\mathscr{F}_{12}|^2+|\mathscr{F}_{23}|^2+|\mathscr{F}_{31}|^2+2\,\mathrm{Re}(\mathscr{F}_{12}\mathscr{F}_{23}\mathscr{F}_{31})]\ . \tag{A11}$$

Further reduction of Eq. (A11) requires the evaluation of two types of integrals:

$$\int dp_3\frac{|f(p_3)|^2}{(2\pi)^3}|\mathscr{F}_{31}|^2=\frac{1}{[1+(p_0R)^2/2]^{3/2}}\exp\left[-\frac{1}{4}p_1{}^2R^2\frac{1}{1+(p_0R)^2/2}\right] \tag{A12}$$

and

$$\int dp_3\frac{|f(p_3)|^2}{(2\pi)^3}\{\mathscr{F}_{23}\mathscr{F}_{31}\}=\frac{1}{[1+(p_0R)^2]^{3/2}}\exp\left[-\frac{1}{2}\frac{(p_1-p_2)^2R^2}{4}\right]\exp\left[-\frac{1}{2}\frac{(p_1+p_2)^2R^2}{1+p_0{}^2R^2}\right]. \tag{A13}$$

In the limit appropriate for a heavy-ion system ($p_0R\gg1$), such terms as those in Eq. (A12) approach a constant (for fixed p_1 or p_2) times $1/(p_0R)^3$, while the second type of term retains a dependence on (p_1-p_2), multiplied by the same inverse phase-space factor. Thus, the two-particle correlation function in a three-particle system is of the form

$$C_{(3)}(p_1,p_2)=1+|\mathscr{F}_{12}|^2+\frac{1}{(p_0R)^3}\left[c_a+c_b\mathscr{F}_{12}\exp\left[-\frac{1}{2}\frac{(p_1-p_2)^2R^2}{4}\right]\right], \tag{A14}$$

where c_a and c_b are constants of order unity. This has the form of the simple two-particle correlation function Eq. (17), modified by a constant term plus a term proportional to c_b with an effective radius smaller by a factor of $\sqrt{3}/2$ than the $|\mathcal{F}_{12}|^2$ term. [Note that since correlation functions defined as in Eq. (16) are normalized by requiring that

$$\lim_{|\mathbf{q}|\gg 1/R} C_2(|\mathbf{q}|)=1 ,$$

the value of λ is determined by the *ratio* of the constant terms to those that depend on p_1-p_2.]

Extension of these arguments to higher pion multiplicities is straightforward; we work in the limit $p_0R\gg 1$: The two-pion correlation function in an n-pion state is proportional to

$$C_2(p_1,p_2) = \int d(p_3,\ldots,p_n)\frac{|f(p_3)|^2}{(2\pi)^3}\cdots\frac{|f(p_n)|^2}{(2\pi)^3}\mathrm{per}\{\mathcal{F}\} . \tag{A15}$$

A general term in the expansion of the permanent contains k factors of the form $\mathcal{F}_{ij}$, $i\neq j$ and $n-k$ factors of $\mathcal{F}_{ii}=1$. The integrals over the $n-k$ momenta all give unity, while the contribution of the remaining k terms depends on the cycle structure of the permutation sequence of their indices. Those cycles which contain both particles 1 and 2 retain a dependence on the quantity p_1-p_2 after all integrations in Eq. (A15) have been performed; all other permutations simply contribute k factors of $1/(p_0R)^3$.

Assume then that the k terms contain a cycle of length l involving both particles 1 and 2, requiring m variables from the set $3,4,\ldots,n$ to go from 1 to 2 and $l-m-2$ more variables to return to 1. Including the $k-l$ integrations over the "unconnected" variables, one can show that the contribution of a term with this structure is given by

$$\left[\frac{1}{(p_0R)^3}\right]^{k+l-2}\exp\left[-\frac{1}{m+1}\frac{R^2}{4}(p_1-p_2)^2\right] \times\exp\left[-\frac{1}{l-m-1}\frac{R^2}{4}(p_1-p_2)^2\right] . \tag{A16}$$

Finally, since $n_{l,m}$, the number of ways to partition l into m and $l-m-2$ integrals, is given by $l!(l-m-2)!$, it is clear most such terms have $m=l-2$, followed by $m=l-3$, and so on. This corresponds to a series of reduced values for the effective radius R_{eff}:

$$\left[\frac{R_{\mathrm{eff}}}{R}\right]^2=\left[\frac{l}{2(m+1)(l-m-1)}\right]\equiv\epsilon_{l,m} , \tag{A17}$$

with $m=0,1,2,\ldots,(l-2)$.

Combining these arguments with that for the number of terms proportional to $\mathcal{F}^k$ [Eq. (12)], it becomes plausible that the correction terms to the two-particle correlation function are an expansion in powers of the phase-space density $\mathcal{N}\equiv n_\pi/(p_0R)^3$. Thus, when $\mathcal{N}\sim 1$, all terms in this expansion are of roughly equal importance, so that the two-particle correlation function becomes a superposition of terms with successively broader distributions in p_1-p_2, leading to an increasingly smaller value for the inferred radius. These successively broader terms also prevent a realistic imposition of the normalization condition for $C_2(|\mathbf{q}|)$, thereby washing out the peak for small $|\mathbf{q}|$ and reducing the effective value of λ.

To estimate a typical reduction in R, we note that the average cycle length for $n_\pi=500$ is about 5. Assume that the reduced R values may be averaged in quadrature (as appropriate for a superposition of Gaussians), so that the average reduction may be written as

$$\langle\epsilon\rangle=\frac{\sum_{m=0}^{m=l-2}\epsilon_{l,m}n_{l,m}}{\sum_{m=0}^{m=l-2}n_{l,m}} . \tag{A18}$$

Evaluating the sum for $l=5$ gives $\langle\epsilon\rangle=0.46$, or $R_{\mathrm{eff}}=0.67R$. The observed reduction of 50% in this quantity is somewhat more than this simple calculation would imply, thereby indicating that higher-order cycles are responsible for the additional reduction. Nonetheless, the rough agreement is a gratifying verification of the validity of these arguments.

*Present address: Department of Physics, Columbia University, New York, NY 10027.

[1]W. Willis and C. Chasman, Nucl. Phys. **A418**, 413 (1984).
[2]B. Andersson and W. Hoffman, Phys. Lett. **169B**, 364 (1986).
[3]T. J. Humanic, Reports Nos. LBL-18679, 1984, LBL-18817, 1985, and LBL-19420, 1985 (unpublished).
[4]W. A. Zajc, in *Proceedings of the RHIC Workshop on Experiments for a Relativistic Heavy Ion Collider*, Upton, New York, 1985, edited by P. E. Haustein and C. L. Woody (BNL-51921, Brookhaven National Laboratory, Upton, NY, 1985).
[5]M. Gyulassy, S. K. Kauffmann, and Lance W. Wilson, Phys. Rev. C **20**, 2267 (1979).
[6]M. Biyajima, Phys. Lett. **92B**, 193 (1980).
[7]P. Edelman (private communication). For a definition and discussion of derangements, see R. Brualdi, *Introductory Combinatorics* (North-Holland, Amsterdam, 1976).
[8]A. Labeyrie, in *Progress in Optics*, edited by E. Wolf (North-Holland, Amsterdam, 1976), Vol. 14.
[9]N. Metropolis *et al.*, J. Chem. Phys. **21**, 1087 (1953).
[10]A. Nijenhuis and H. S. Wilf, *Combinatorial Algorithms*, 2nd ed. (Academic, New York, 1978).
[11]D. Ceperley, G. V. Chester, and M. H. Kalos, Phys. Rev. B **17**, 1070 (1978).
[12]G. Goldhaber *et al.*, Phys. Rev. **120**, 300 (1960).
[13]Brookhaven National Laboratory Report No. BNL-51801,

1984 (unpublished).

[14]See, e.g., I. Otterlund, Nucl. Phys. **A418**, 87 (1984).

[15]K. Kolehmainen and M. Gyulassy, Phys. Lett. **180B**, 203 (1986).

[16]By reducing the radius and pion multiplicity such that the phase-space density remains constant, we have verified that the observed large distortions depend essentially on the density, rather than the pion number. While the available computing resources did not permit an extensive investigation of pion number versus pion density, we note that this result is as expected from second-order stellar interferometry, where the local phase-space density is the relevant parameter, not the (extraordinarily high) photon numbers.

[17]All execution times refer to FORTRAN programs operating on an IBM 3081-G running under VM/CMS. These times should not be regarded as optimized values, but rather as indicative of a FORTRAN program with some substantial overhead involving histogramming and diagnostics.

[18]Particle Data Group, Rev. Mod. Phys. **56**, S1 (1984).

[19]Y. M. Liu *et al.*, Phys. Rev. C **34**, 1667 (1986).

[20]G. Goldhaber, in *Local Equilibrium in Strong Interaction Physics*, proceedings of the First Workshop, Bad Honneff, West Germany, 1984, edited by D. K. Scott and R. M. Weiner (World Scientific, Singapore, 1985).

[21]M. Biyajima, Prog. Theor. Phys. **66**, 1378 (1981); **68**, 1273 (1981).